Journal of Medicinal Chemistry Article

J. Med. Chem. **2010,** *53,* 7405–7413 **7405**
DOI: 10.1021/jm100565d

Antidiabetic and Antiobesity Effects of Ampkinone (6f), a Novel Small Molecule Activator of AMP-Activated Protein Kinase

Sangmi Oh,[†] Sung Jin Kim,[§,∥] Jung Hwan Hwang,[⊥] Hyang Yeon Lee,[†] Min Jeong Ryu,[§,∥] Jongmin Park,[†] Soung Jung Kim,[§,∥] Young Suk Jo,[§,∥] Yong Kyung Kim,[§,∥] Chul-Ho Lee,[⊥] Ki Ryang Kweon,[∥] Minho Shong,*[,§,∥] and Seung Bum Park*[,†,‡]

[†]*Department of Chemistry,* [‡]*Department of Biophysics and Chemical Biology, Seoul National University, Seoul 151-747, Korea,* [§]*Department of Internal Medicine, and* [∥]*Department of Biochemistry, Chungnam National University School of Medicine, Daejeon 301-721, Korea, and* [⊥]*Laboratory of Experimental Animals, Korea Research Institute of Bioscience and Biotechnology (KRIBB), Daejeon 305-806, Korea*

Received May 10, 2010

Adenosine 5'-monophosphate (AMP) activated protein kinase (AMPK) has emerged as an attractive target molecule for the treatment of metabolic disorders, including obesity and type 2 diabetes. In this study, we identified a novel small molecule, ampkinone (**6f**), as an indirect AMPK activator, which was derived from the small molecule library constructed by diversity-oriented synthesis. Ampkinone stimulated the phosphorylation of AMPK via the indirect activation of AMPK in various cell lines. Ampkinone-mediated activation of AMPK required the activity of LKB1 and resulted in increased glucose uptake in muscle cells. In addition, ampkinone-treated DIO mice significantly reduced total body weight and overall fat mass. Histological examination and measurement of lipid parameters showed that ampkinone effectively improved metabolic abnormalities in the DIO mice model. Our results demonstrate that ampkinone, a small molecule with a privileged benzopyran substructure, has a potential as a new class of therapeutic agent for antidiabetic and antiobesity treatment via the indirect stimulation of AMPK.

Introduction

The global incidence of type 2 diabetes is increasing rapidly, with higher rates of morbidity and mortality, resulting in a significant financial and social burden worldwide.[1] Type 2 diabetes is characterized by insulin resistance and hyperglycemia, which lead to chronic complications in both small and large blood vessels.[2,3] Therefore, numerous studies have focused on the development of therapeutics able to maintain normal levels of blood glucose by increasing glucose clearance in peripheral tissues such as skeletal muscle and adipose tissue.[4,5] Recent studies have shown that impaired handling of cellular energy homeostasis is closely associated with insulin resistance, resulting in type 2 diabetes, metabolic syndrome, hypertension, and increased cardiovascular risk.[6] Therefore, molecules that regulate cellular energy metabolism hold promise as drug targets for the development of therapeutics for diabetes and obesity.[7]

AMP[a]-activated protein kinase (AMPK) is a heterotrimeric complex comprising catalytic α and regulatory β/γ subunits that senses low energy status by monitoring the ratio of ATP to AMP.[8] AMPK is activated during muscle contraction and exercise by the phosphorylation of threonine 172 by LKB1[9] and Ca^{2+}/calmodulin-dependent kinase kinase (CaMKK).[10] Once AMPK is activated, it stimulates glucose uptake in skeletal muscle through independent pathways in insulin-resistant conditions.[11] Enhanced glucose uptake induced by AMPK is achieved, as least in part, by enhanced GLUT4 translocation to the plasma membrane for fusion and docking.[12] Several studies have reported that the AMP analogue, 5-aminoimidazole-4-carboxamide-1-β-D-ribofuranoside (AICAR), and other small-molecule activators of AMPK increase glucose uptake in vitro[13] and in vivo.[14] Although their mechanisms of action are still incompletely understood, evidence indicates that metformin[15] and thiazolidinediones (TZDs)[16] act through activation of AMPK in type 2 diabetes. Furthermore, AMPK is the target molecule of two adipose tissue-derived hormones, leptin[17] and adiponectin,[18] which are major regulators of energy metabolism and glucose homeostasis. These accumulated findings have made AMPK an attractive therapeutic target for the treatment of type 2 diabetes and obesity.

In this study, we identified a small-molecule activator of AMPK, ampkinone (**6f**), as an effective therapeutic agent for the treatment of obesity and type 2 diabetes. This novel skeleton (**6**) is a tetracyclic structure embedded with a privileged benzopyran substructure, derived from 2500-member small molecules library constructed in-house using diversity-oriented synthesis strategy to prepare skeletally diverse small molecules to mimic natural product-like or druglike chemical structures.[19] This collection of druglike small molecules containing more than 40 unique molecular frameworks can increase the possibility of identifying a novel modulator of biological system such as AMPK.[20] Ampkinone, a small molecule with this molecular

*To whom correspondence should be addressed. For M.S.: phone, (+)82-42-280-7161; fax, (+)82-42-280-7995; e-mail, minhos@cnu.ac.kr. For S.B.P.: phone, (+)82-2-880-9090; fax, (+)82-2-884-4025; e-mail, sbpark@snu.ac.kr.

[a] Abbreviations: AMP, adenosine 5'-monophosphate; AMPK, adenosine 5'-monophosphate activated protein kinase; AKN, ampkinone; CaMKK, Ca^{2+}/calmodulin-dependent kinase kinase; DIO, diet-induced obese; GLUT4, glucose transporter 4; AICAR, 5-aminoimidazole-4-carboxamide-1-β-D-ribofuranoside; TZDs, thiazolidinediones; ACC, acetyl-CoA carboxylase; DOS, diversity-oriented synthesis; DDQ, 2,3-dichloro-5,6-dicyanobenzoquinone; SAR, structure−activity relationship; CLSM, confocal laser scanning microscopy; IPGTT, intraperitoneal glucose tolerance test; ITT, insulin tolerance test; NEFA, nonesterified fatty acids; HMG-CoA, 3-hydroxy-3-methylglutaryl coenzyme A.

Published on Web 09/28/2010

framework (**6**), stimulated the activation and phosphorylation of AMPK in cell lines originating from muscle, fat, and liver. Phosphorylation of acetyl-CoA carboxylase (ACC), a major downstream target molecule of AMPK, confirmed that ampkinone stimulates functional activation of AMPK via the phosphorylation at Thr172 in cultured cells. We also demonstrated the enhanced cellular glucose uptake monitored by fluorescent glucose bioprobe, Cy3-Glc-α,[21] and cross-checked with ^{3}H-labeled 2-deoxy-D-glucose. Consistent with the in vitro data presented here, administration of ampkinone to diet-induced obese (DIO) mice up-regulated the activity of AMPK in the liver and muscle and enhanced insulin sensitivity. Furthermore, histological analysis confirmed that ampkinone treatment accelerated the consumption of lipids via increased oxidation in the liver and adipose tissues, similar to other small molecule activators of AMPK.[22] Collectively, the results demonstrate that ampkinone is a new small-molecule activator of AMPK that may be effective for the treatment of type 2 diabetes and obesity.

Results and Discussion

Identification of Ampkinone, a Novel Small-Molecule Activator of AMPK. We previously reported synthetic methods for the concise and efficient library construction using diversity-oriented synthesis (DOS) strategy, which generated novel scaffolds embedded with privileged substructures via various chemical transformations.[20] To identify a novel small-molecule activator of AMPK, we evaluated an in-house small molecule collection constructed by these DOS pathways. After extensive bioassays using Western blot analysis, we identified a new molecular framework (**6**) that stimulates the phosphorylation of AMPK. The aromatized benzopyran moiety in **6** was shown to be essential for AMPK activation because other types of benzopyran-fused tetracycles such as monoene (**5**), hydrogenated compound (**S7**), and allylic alcohol (**S8**) were inactive toward AMPK (Figure S1 of Supporting Information). On the basis of initial screening results, a focused small molecule library was constructed by a series of reactions designed to produce **6**: [1] the cyclization of hydroxyacetophenones (**1**) with acetone or cyclopentanone, [2] triflation of carbonyl moiety on substituted chroman-4-ones (**2**), [3] palladium-mediated vinylation of vinyl triflate intermediates (**3**), [4] Diels−Alder reaction of bicyclic dienes (**4**) with substituted maleimides, and [5] subsequent aromatization of benzopyran-containing tetracyclic monoenes (**5**) with 2,3-dichloro-5,6-dicyanobenzoquinone (DDQ) (Scheme 1).

Using a 15-member focused library (**6a**−**o**) with various structural modifications, we conducted a structure−activity relationship (SAR) study via Western blot analysis (see Table 1). On the basis of our SAR study, 2-(4-benzoylphenyl)-6-hydroxy-7-methoxy-4,4-dimethylchromeno[3,4-*e*]isoindole-1,3-dione (**6f**) demonstrated the most efficient activation of AMPK and subsequent functional phosphorylation of ACC (Figure S2). The compound activity on AMPK phosphorylation was slightly attenuated when benzophenone moiety at the R^3 position of molecular framework **6** was replaced with simpler moieties such as acetylphenyl group (**6e**) and phenyl (**6c**), but it was completely abolished when hydrogen (**6a**), methyl (**6b**), and benzyl group (**6d**) were introduced at the R^3 position. The introduction of bulky substituents such as biphenyl-4-yl (**6g**), biphenyl-3-yl (**6i**), and 4-benzylphenyl group (**6j**) diminished the activity in Western blot analysis; however, 9-oxo-9*H*-fluoren-3-yl moiety (**6h**) somewhat preserved its activity because of its structural similarity to benzophenone. In addition, cyclopentyl moiety at the R position

Scheme 1. Synthetic Scheme of Benzopyran-Embedded Molecular Framework (**6**)[a]

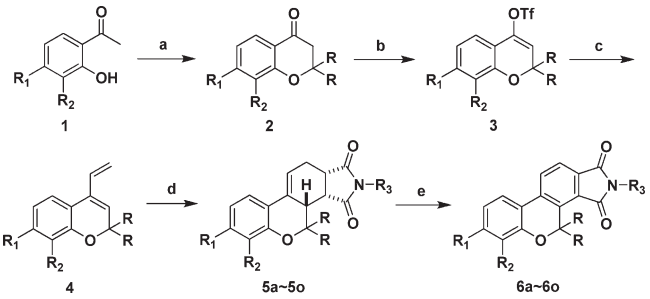

[a] Reagents and conditions: (a) cyclopentanone or acetone, pyrrolidine, EtOH, reflux; (b) trifluoromethanesulfonic anhydride, 2,6-di-*tert*-butyl-4-methylpyridine, CH_2Cl_2, 0 °C; (c) vinylboronic acid dibutyl ester, $Pd(PPh_3)_4$, Na_2CO_3, EtOH/toluene/H_2O, 70 °C; (d) maleimide derivatives, toluene, reflux; (e) DDQ, toluene, reflux.

Table 1. Activation of AMPK (pT172) and ACC (pS79) phosphorylation induced by individual compounds in the focused library

Cpd.	R	R^1	R^2	R^3	% activity[a]	
					AMPK	ACC
6a	Me	OMe	OH	H	158	123
6b	Me	OMe	OH	Me	205	145
6c	Me	OMe	OH	Ph	273	254
6d	Me	OMe	OH	Bn	165	194
6e	Me	OMe	OH	*p*-Acetylphenyl	264	384
6f	Me	OMe	OH	4-Benzoylphenyl	322	295
6g	Me	OMe	OH	Biphenyl-4-yl	160	114
6h	Me	OMe	OH	9-Oxo-9*H*-fluoren-3-yl	249	154
6i	Me	OMe	OH	Biphenyl-3-yl	175	201
6j	Me	OMe	OH	4-Benzylphenyl	169	129
6k	Me	OMe	OH	4-(Benzo[*d*]oxazol-2-yl)phenyl	92	91
6l	Me	OMe	H	4-Benzoylphenyl	159	154
6m	Me	F	H	4-Benzoylphenyl	186	156
6n	Me	H	H	4-Benzoylphenyl	203	92
6o	$-(CH_2)_4-$	OMe	OH	4-Benzoylphenyl	113	51

[a] Relative phosphorylation activity induced by the treatment of individual compounds at 10 μM in the Western blot analysis.

(**6o**) or various substituents at the R^1 and R^2 positions (**6l**−**n**) caused a significant reduction in the compound activity on AMPK phosphorylation. On the basis of this screening result, we classified **6f** as a novel small molecule activator of AMPK and designated this compound ampkinone (AKN) (Figure 1A).

AKN Stimulates Phosphorylation of AMPK in Muscle-, Adipose-, and Liver-Derived Cell Lines in a Dose- and Time-Dependent Manner. To investigate the effect of AKN on AMPK activation, we utilized cell lines originating from cardiac and skeletal muscle, adipose tissue, and liver. Immunoblot analysis of a time course assay conducted in L6 skeletal muscle cells revealed that the AKN-mediated phosphorylation of AMPK (Thr172) was increased at 10 min, reached a maximum at 1 h, and persisted for 6 h (Figure 1B). Phosphorylation of ACC (Ser79), an intracellular substrate of AMPK, was also increased by treatment with AKN on a timeline similar to that of AMPK. Immunocomplex kinase assays with the SAMS peptide revealed a 2.7-fold increase in AMPK activity upon treatment with 10 μM AKN. Treatment with 1 mM AICAR as a positive control for AMPK activation induced a 3.2-fold increase in AMPK activity (Figure 1C). We next examined the dose-dependent effect of AKN on AMPK activation. The phosphorylation of AMPK and ACC was dose-dependently increased in various cell lines, such as C2C12 skeletal muscle cells, 3T3-L1 adipose-like mouse embryonic fibroblasts, and

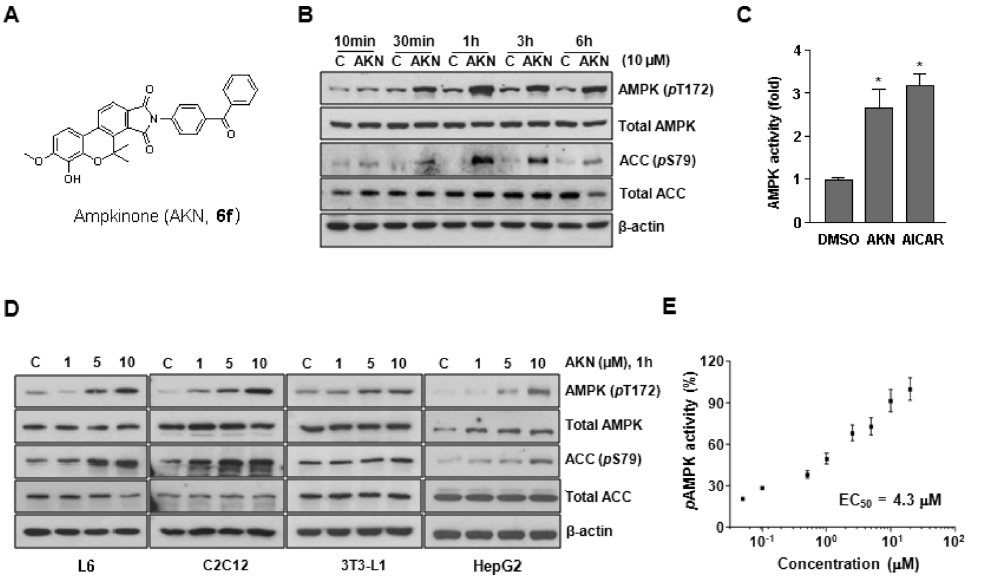

Figure 1. AKN stimulates the phosphorylation of AMPK (pT172) and ACC (pS79) in a time- and dose-dependent manner. (A) Chemical structure of AKN (**6f**). (B) AKN-induced phosphorylation of AMPK (pT172) and ACC (pS79). Western blot analysis of lysates from L6 cells treated with AKN (10 μM) for the indicated times was performed with antibodies against the indicated proteins. (C) Total AMPK activity in cells treated with AKN or DMSO was measured using a synthetic SAMS peptide substrate and [γ-^{32}P]ATP. (D) L6 cells, C2C12 myocytes, 3T3-L1 preadipocytes, and HepG2 hepatic cells were incubated for 1 h with the indicated concentrations of AKN. (E) EC_{50} was determined by Western blotting in various concentrations (0−20 μM) and data analysis with PRISM3 program. Immunoblots were performed using anti-AMPK (pT172), anti-AMPK, anti-ACC (pS79), and anti-ACC antibodies. (*) $P < 0.05$ vs corresponding control.

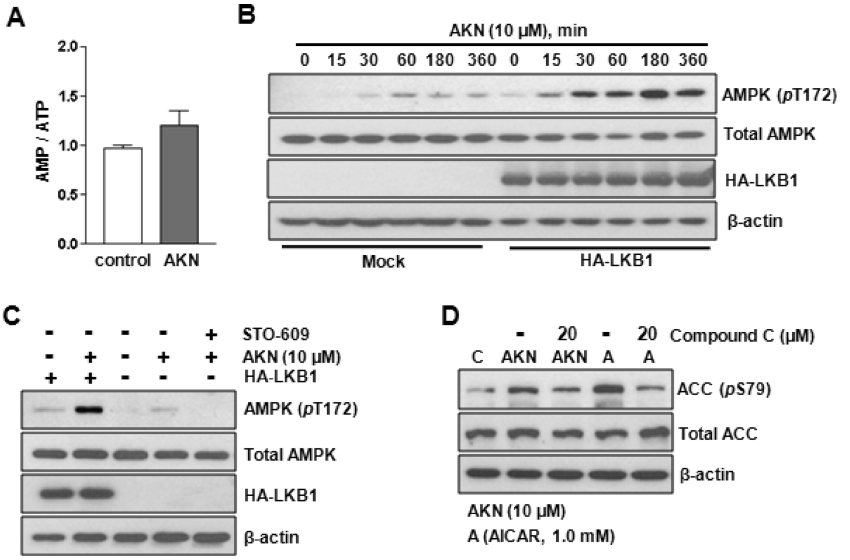

Figure 2. AKN predominantly stimulates AMPK activation via the LKB1 pathway. (A) AMP to ATP ratio was not significantly changed upon treatment with AKN. (B) LKB1-deficient HeLa cells and HeLa cells transfected with a pcDNA3.1 plasmid encoding LKB1-tagged hemagglutinin (HA) were exposed to AKN (10 μM) for the indicated time periods after 6 h of serum starvation. Immunoblot analysis was then performed with antibodies against AMPK (pT172), AMPK, and HA. (C) The effect of the CaMKK inhibitor, STO-609, on AKN-mediated AMPK activation following 1 h of treatment in Hela cells. (D) L6 cells were exposed to AKN (10 μM) or AICAR (1 mM) for 1 h in the presence or absence of compound **C** (20 μM), and immunoblots were performed with anti-ACC (pS79), anti-ACC, and anti-actin as a loading control.

HepG2 human hepatoma cells as well as L6 cells (Figure 1D). These data indicate that AKN stimulates the phosphorylation and activity of AMPK in multiple cell lines originating from muscle, fat, and liver. The estimated EC_{50} of AKN is 4.3 μM in L6 cells (Figure 1E and Figure S3).

AKN-Mediated AMPK Phosphorylation Requires the Upstream Kinases, LKB1 and CaMKK. We next determined whether AKN could directly activate AMPK. ^{32}P incorporation by isolated AMPK into the SAMS peptide was not different in AKN-treated samples compared to the DMSO control (data not shown). This suggests that AKN does not directly activate purified AMPK in a cell-free condition. Then we investigated whether the cellular levels of AMP, ADP, or ATP can be perturbed upon treatment with AKN. As shown in Figure 2A, the treatment with AKN at 10 μM caused no significant alteration in AMP to ATP ratio in L6 cells (Figure S4).

Consequently, we hypothesized that AKN might stimulate AMPK phosphorylation through the activation of upstream signaling pathway. LKB1 and CaMKK are two primary AMPK

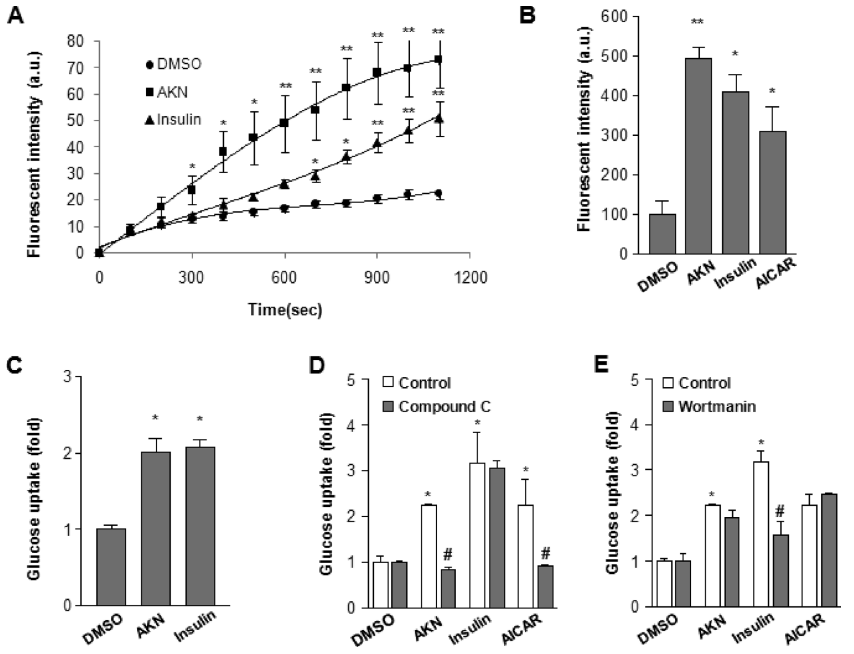

Figure 3. AKN stimulates glucose uptake through AMPK but not Akt. (A) C2C12 and (B) L6 myocytes were incubated for 1 h with AKN (10 μM) or insulin (100 nM). Next, (A, B) Cy3-Glc-α (DMSO-treated = closed circles; AKN-treated = closed squares; insulin-treated = closed triangles) or (C) 2-deoxy-D-glucose-1,2-^{3}H(N) was added to culture media for the indicated time periods (A) or 10 min (B, C), and glucose uptake was measured. (D) The effect of the AMPK inhibitor compound **C** (20 μM, 30 min preincubation) and (E) the PI3K inhibitor wortmannin (1 μM, 30 min preincubation) on AKN- (10 μM), insulin- (100 nM), or AICAR (1 mM)-mediated glucose uptake following 1 h of treatment in L6 myocytes: (*) $P < 0.05$; (**) $P < 0.01$ vs corresponding control; (#) $P < 0.05$ vs corresponding treated groups (AKN, insulin, and AICAR).

kinases.[9,10] For the mechanistic understanding, we investigated whether one or both of these kinases were required for the activation of AMPK by AKN. As confirmed by the data shown in Figure 2B, HeLa cells do not express LKB1.[23] Therefore, HeLa cells were transfected with hemagglutinin (HA)-tagged LKB1 for 24 h to induce the expression of exogenous LKB1 and then treated with AKN for the indicated time. In mock-transfected cells, treatment with AKN slightly increased AMPK phosphorylation from 60 to 360 min, while AMPK phosphorylation in LKB1-transfected cells was noticeably higher. These data indicate that LKB1 activity is required for robust AKN-mediated AMPK phosphorylation, though the slight increase in AMPK phosphorylation in mock-transfected cells suggested the involvement of another upstream kinase. Accordingly, HeLa cells were preincubated with STO-609, a specific inhibitor of CaMKK.[24] Treatment of STO-609 in mock-transfected HeLa cells completely suppressed the phosphorylation of AMPK induced by AKN (Figure 2C), indicating that LKB1 and CaMKK mediate the activation of AMPK by AKN. Finally, to determine whether phosphorylation of ACC upon treatment with AKN is associated with AMPK, L6 cells were preincubated with the AMPK-specific inhibitor, compound **C**, followed by treatment with AKN for 1 h. As shown in Figure 2D, AKN-induced ACC phosphorylation was significantly diminished through the specific inhibition of AMPK with compound **C**. Taken together, these data confirm that AKN stimulates the phosphorylation of AMPK neither by direct activation as in the case of AICAR, an AMP analogue, nor by the consequence of altered cellular AMP/ATP ratio. In addition, it was also confirmed that both kinases, LKB1 and CaMKK, are required for full activation of AKN-stimulated phosphorylation of AMPK.

AKN Increases the Cellular Uptake of Glucose in C2C12 and L6 Myocytes. AMPK plays a crucial role as an energy sensor in metabolic tissues and stimulates glucose uptake in skeletal muscle.[8] To determine the effect of AKN on cellular glucose uptake, we utilized the fluorescent glucose bioprobe, Cy3-Glc-α, which enters the cell through competition with D-glucose via glucose transporters (GLUTs) (Figure S5).[21] Compared to glucose uptake assay with radioisotope-labeled deoxy-D-glucose using scintillation counter, this method allows the real-time monitoring of cellular glucose uptake under experimental conditions using fluorescent microscopy or confocal laser scanning microscopy (CLSM). As shown in Figure 3A, a 2.3-fold enhancement in cellular glucose uptake was observed by CLSM in C2C12 myocytes treated with insulin. Under identical experimental settings, we measured a 3.2-fold enhancement in cellular glucose uptake upon treatment with AKN. Enhanced cellular glucose uptake was also monitored by fluorescent microscopy following treatment with AKN, insulin, and AICAR (Figure 3B and Figure S6), and a dose-dependent enhancement of fluorescent intensity was observed in cells treated with AKN (Figure S7). These data were confirmed by the conventional glucose uptake assay with 2-deoxy-D-glucose-1,2-^{3}H(N) using scintillation counter (Figure 3C).

Insulin-dependent PI3K/Akt signaling and insulin-independent AMPK signaling are two of the pathways that regulate cellular glucose uptake.[25] To understand the cellular mechanisms underlying this process, we investigated the involvement of both pathways in AKN-enhanced glucose uptake by inhibiting either the AMPK pathway or the PI3K/Akt pathway with compound **C** and wortmannin, respectively. Cellular glucose uptake was stimulated by AKN, AICAR, and insulin in C2C12 myocytes. The inhibition of AMPK with compound **C** resulted in a complete inhibition of enhanced glucose uptake in cells treated with AKN and AICAR (Figure 3D). However, the enhanced glucose uptake induced by insulin was not affected by the inhibition of

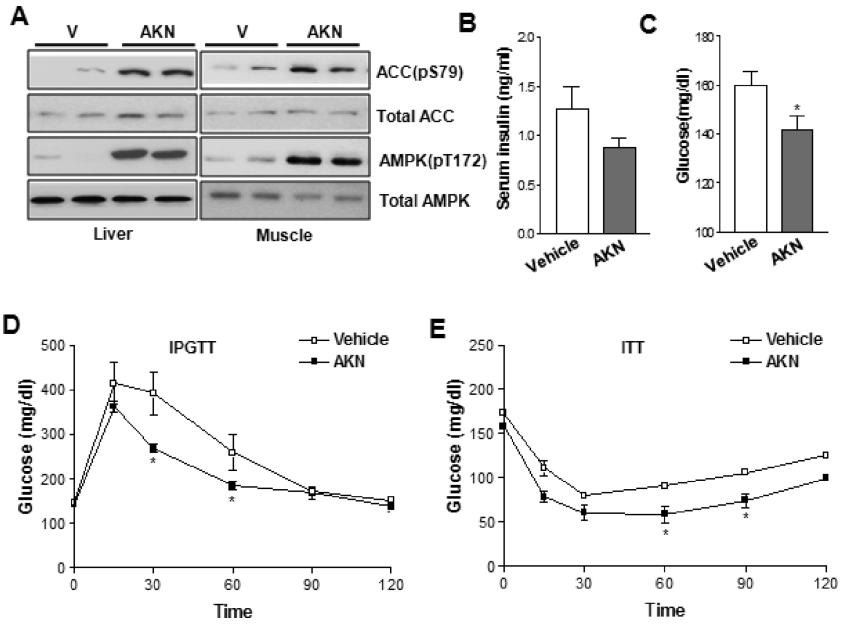

Figure 4. AKN activates the AMPK signaling pathway and enhances glucose homeostasis in vivo. (A) The effect of AKN on the phosphorylation of AMPK and ACC in vivo. Vehicle (PEG400, $n = 7$) or 10 (mg/kg)/d AKN ($n = 7$) were administered subcutaneously to DIO mice. After administration of AKN for 1 month, immunoblot analysis of tissue lysates from liver and muscles was performed with antibodies against the indicated proteins after fasting for 24 h. (B) Serum insulin and (C) blood glucose levels were determined using the ALPCO insulin EIA kit and a glucometer (Accu Check, Roche), respectively. (D) The intraperitoneal glucose tolerance test (IPGTT) and (E) insulin tolerance test (ITT) were performed in DIO mice treated with vehicle (□, $n = 7$) or 10 (mg/kg)/d AKN (■, $n = 7$) for 3 weeks and 4 weeks, respectively: (∗) $P < 0.05$; (∗∗) $P < 0.01$ vs the corresponding vehicle control group.

AMPK. In contrast, the glucose uptake pattern in insulin-treated cells was reversed only after pretreatment with wortmannin (Figure 3E). Consistent with this data, immunoblot analysis revealed that Akt phosphorylation was not increased above basal levels by treatment with AKN (Figure S8). This demonstrates that AKN-stimulated glucose uptake results primarily from increased AMPK activation and not via PI3K/Akt signaling.

AKN Enhances Glucose Dispersal and Insulin Sensitivity via Activation of AMPK in Vivo. We next examined the in vivo effect of AKN in DIO mice fed a diet containing 60% fat for 8 weeks after microsomal stability test of this compound (Figure S9). DIO mice were injected subcutaneously for 4 weeks with 10 (mg/kg)/d of AKN in PEG400. Phosphorylation of AMPK was confirmed by immunoblot analysis of proteins from the liver and muscle of DIO mice treated with vehicle or AKN. Consistent with our in vitro data, AKN-treated DIO mice had increased levels of phosphorylated AMPK/ACC, suggesting that AKN is an effective activator of AMPK in liver and muscle (Figure 4A). Interestingly, we observed that serum insulin and glucose levels in AKN-treated DIO mice were lower than those in the control groups (Figure 4B and Figure 4C). Therefore, we investigated the glucose dispersal rates in both groups. As shown in Figure 4D, elevated blood glucose induced by intraperitoneal injection was more rapidly lowered in AKN-treated DIO mice than control mice. These findings indicate that AKN effectively enhanced insulin sensitivity in animal models (Figure 4E). Taken together, these data support that AKN is a novel small-molecule AMPK activator with antidiabetic effects.

AKN Accelerates the Consumption of Accumulated Fat in DIO and Reduces Total Body Weight. We next sought to investigate the potential antiobesity effects of AKN. AKN (10 (mg/kg)/d) was administered to DIO mice for 30 days via subcutaneous injection, and food intake and body weight were monitored every 3 days. No significant difference in food intake was observed between the groups (Figure 5A). Interestingly, by week 3, the body weights of AKN-treated DIO mice were significantly decreased, resulting in a ~5% decrease compared to the initial weight. Conversely, the weights of vehicle-treated DIO mice increased slightly over the study period (Figure 5B). The changes in body weight were the result of changes in fat mass, which were significantly decreased in AKN-treated mice compared to vehicle-treated mice (Figure 5C). In agreement with this observation, Oil-red O staining of liver and H & E staining of gonadal fat revealed dramatic differences between AKN- and vehicle-treated mice in terms of fat mass and fat area, respectively (Figure 5D). Finally, although triglyceride levels in serum were not affected upon treatment with either AKN or vehicle (Figure 5F), other lipid parameters such as cholesterol and nonesterified fatty acids (NEFA) were significantly decreased in AKN-treated DIO mice compared to control groups (Figure 5E and 5G). These data indicate that AKN also has antiobesity effects.

Conclusion

In this paper, we have described ampkinone, a novel small-molecule activator of AMPK with potential antidiabetic and antiobesity effects. Through extensive immunoblotting assays using a 2500-member small molecule collection constructed by diversity-oriented synthesis strategy,[20] we identified a novel molecular framework (**6**) with a privileged benzopyranyl substructure. We then conducted a structure−activity relationship (SAR) study using a 15-member focused library with a tetracyclic skeleton (**6**) and identified **6f** as the best candidate for further in vitro and in vivo evaluation. This compound, which we designated ampkinone (AKN), is an effective small-molecule activator of AMPK. We confirmed the in vitro effects of AKN on the functional activation of AMPK through active phosphorylation of

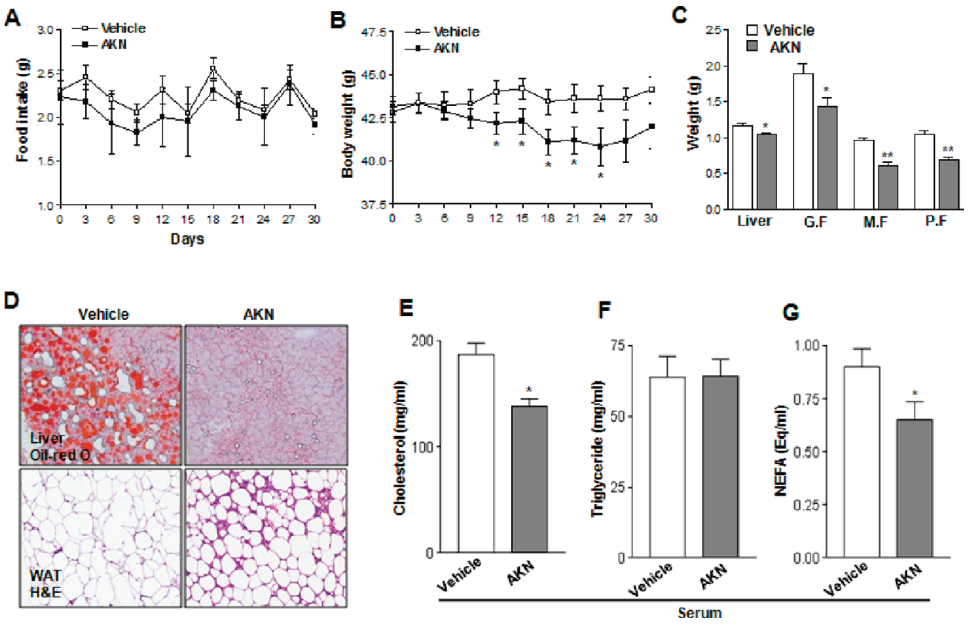

Figure 5. AKN treatment ameliorates metabolic symptoms in DIO mice. (A) Food intake and (B) the body weight of DIO mice groups, either vehicle-treated (□, $n = 7$) or AKN-treated (■, $n = 7$), were monitored during the subcutaneous administration of 10 (mg/kg)/d AKN for 1 month. (C) The weights of adipose tissues (GF, gonadal fat; MF, mesenteric fat; PF, perirenal fat) and other organs were compared between DIO mice treated with vehicle (□, $n = 7$) and those treated with 10 (mg/kg)/d AKN (■, $n = 7$) for 1 month. (D) Oil-red O staining of liver cells from DIO mice treated with vehicle (upper, left) or 10 (mg/kg)/d AKN (upper, right) and H & E staining of gonadal fat from DIO mice treated with vehicle (lower, left) or 10 (mg/kg)/d AKN (lower, right). (E−G) Lipid parameters of serum from DIO mice after subcutaneous administration of vehicle (□, $n = 7$) or 10 (mg/kg)/d AKN (■, $n = 7$) for 1 month: (∗) $P < 0.05$; (∗∗) $P < 0.01$ vs the corresponding vehicle control group.

ACC, its specific substrate, in multiple cell lines derived from metabolic tissues.

AMPK is an important energy sensor in mammalian cells. Its activity is induced in response to high levels of AMP and/or low ATP. Under these conditions, AMP binds to the γ-subunit of AMPK and induces a conformational change that allows Thr172 of the α-subunit to be phosphorylated by AMPK kinases.[8] AMPK is activated by upstream kinases, including LKB1[9] and CaMKK.[10] We determined that both kinases, LKB1 and CaMKK, are required for full activation of AKN-stimulated phosphorylation of AMPK. On the basis of our findings in LKB1- and mock-transfected HeLa cells, AKN-mediated AMPK activation was induced mainly via the up-regulation of LKB1. Although AKN-mediated AMPK phosphorylation is primarily mediated by LKB1, the activation of AMPK is also slightly stimulated by CaMKK upon treatment of AKN evidenced by immunoblot analysis with specific inhibitors. Both LKB1 and CaMKK function as AMPK kinases in different cell lines and tissues, suggesting that they play different roles in the regulation of AMPK. However, the molecular mechanism of AKN-mediated AMPK activation remains to be elucidated.

It has been well established that activation of AMPK stimulates glucose uptake by increasing GLUT4 translocation to the cell surface.[26] Interestingly, AMPK-mediated glucose uptake occurs through a different mechanism than in the insulin-signaling pathway.[27] As shown in Figure 3, AKN strongly increased glucose uptake in C2C12 myocytes. This effect was completely eliminated by the inhibition of AMPK with compound **C** but not by the inhibition of PI3K via wortmannin. In addition, AKN treatment did not induce phosphorylation of Akt in L6 cells. These data suggest that AKN-mediated glucose uptake is dependent on AMPK, not Akt. In addition, our results demonstrated that AKN does not induce cell cycle arrest or associated cell apoptosis even after strong activation of AMPK for 6 h, which was confirmed by cell viability assays (Figures S10 and S11). Furthermore, OXPHOS activity in L6 myocytes was not affected by treatment with AKN, indicating that AKN-mediated AMPK activation did not result from inhibition of the respiratory chain.[28] Therefore, AKN could be ideal for investigating the physiological effects of AMPK up-regulation without causing oxidative stress.

Abnormal AMPK activity has been implicated in the progression of obesity and diabetes.[8] Several reports suggest that activation of AMPK enhances insulin sensitivity and increases glucose cellular uptake in vitro and in vivo.[4,5,7] In this study, activation of AMPK by AKN enhanced insulin sensitivity and induced glucose uptake in various cultured cell lines and DIO mice, resulting in a reduction in serum insulin and glucose levels (Figure 4). Moreover, the activity of ACC, a key enzyme in lipid accumulation and synthesis, is negatively regulated by activation of AMPK. Similar to other AMPK stimulators,[16,29] AKN treatment resulted in a mild reduction in body weight and a concomitant reduction in adipose tissue weight. Furthermore, hepatic steatosis can result from abnormal activity of 3-hydroxy-3-methylglutaryl coenzyme A reductase (HMG-CoA reductase) and ACC. These two enzymes are regulated by AMPK and primarily responsible for hepatic cholesterol and fatty acid synthesis.[30] Our data suggested that AKN-mediated AMPK activation in DIO mice leads to a reduction in hepatic steatosis and decreased cholesterol and free fatty acids in the serum. However, we need to identify the real target protein regulating AKN-mediated AMPK activation in order to understand the exact regulating mechanism of these antidiabetic and antiobesity effects found in vitro and in vivo. Overall, our results demonstrate that the small-molecule AKN indirectly stimulates the activation of AMPK and has a potential as a therapeutic agent for the treatment of diabetes and obesity.

Experimental Section

Chemical Synthesis. All compounds were synthesized from commercially available starting materials, 2-hydroxyacetophenone derivatives, and the purity of each compound was over 95%. See Supporting Information for details.

Compound 6f, Ampkinone. Yellow solid (62% from compound **5f**). ^{1}H NMR (500 MHz, $CDCl_3$): δ 8.04 (d, J = 8.0 Hz, 1H), 7.96 (d, J = 8.5 Hz, 2H), 7.93 (d, J = 8.0 Hz, 1H), 7.85 (d, J = 7.5 Hz, 2H), 7.64−7.60 (m, 3H), 7.51 (t, J = 7.5 Hz, 2H), 7.20 (d, J = 8.5 Hz, 1H), 6.67 (d, J = 8.5 Hz, 1H), 5.52 (s, 1H), 3.96 (s, 3H), 2.00 (s, 6H). ^{13}C NMR (125 MHz, $CDCl_3$): δ 195.9, 166.8, 166.4, 149.4, 140.6, 140.1, 137.6, 137.2, 137.0, 135.6, 135.1, 132.9, 131.4, 131.1, 130.3, 128.6, 128.0, 127.1, 126.4, 123.7, 115.1, 114.8, 105.8, 80.3, 56.5, 27.3. HRMS (FAB) m/z calculated for $C_{31}H_{24}NO_6$ $[M + H]^+$: 506.1603. Found: 506.1604.

Animal Models. All animals were maintained and used in accordance with the guidelines of the Institutional Animal Care and Use Committee of the Chungnam National University School of Medicine. C57BL/6J mice were obtained from the Jackson Laboratory and housed individually in a room maintained at 25 °C on a 12/12 h light/dark schedule. For diet-induced obesity (DIO) mice, 4-week-old male C57BL/6J mice were fed a high-fat diet (HFD, Research Diets, 60% calories from fat) ad libitum for 8 weeks. Ampkinone in polyethylene glycol (PEG400) or vehicle was administered subcutaneously at 10 mg/kg body weight per day for 1 month. Body weight and food intake were measured every 3 days. All animals were given an insulin tolerance test (ITT) and sacrificed at 30 days. Liver weight and fat masses were measured, sectioned, and stained with Oil-red O and H&E.

Antibodies and Reagents. Antibodies against total AMPK, phospho-AMPK (Thr172), total ACC, phospho-ACC (Ser79), total Akt, and phospho-Akt (Ser473) were purchased from Cell Signaling Technology (Beverly, MA). Antibodies against AMPK-α1 and AMPK-α2 were obtained from Upstate Biotechnology (Lake Placid, NY). The AMPK activator, AICAR, and the AMPK inhibitor, compound **C**, were purchased from Merck Research Laboratories (NJ). 2-Deoxy-D-glucose-1,2-^{3}H(N) (25−50 Ci/mmol) and adenosine 5′-triphosphate, [γ-^{32}P] (3000 Ci/mmol) were purchased from PerkinElmer Inc. (Shelton, CT), and STO-609 was purchased from Calbiochem (La Jolla, CA). All cell culture media and supplements were obtained from Gibco-BRL Life Technologies (Gaithersburg, MD). All other reagents were purchased from Sigma Chemical Co. (St. Louis, MO).

Cell Culture. L6 muscle cells and all cell lines were cultured in Dulbecco's modified Eagle medium (DMEM) containing 10% fetal bovine serum (FBS) and antibiotic solution (100 units/mL penicillin, 100 g/mL streptomycin) at 37 °C in an atmosphere of 5% CO_2 and 95% air. Plasmids containing the recombinant *HA-LKB1* gene were transfected using Lipofectamin and Lipofectamin Plus (Invitrogen) according to the manufacturer's instructions. Cells were grown to 70% confluence and deprived of serum for 6 h prior to treatments. Differentiation of L6 and C2C12 myocytes was induced by DMEM supplemented with 2% horse serum, and the medium was replaced every 2 days.

Immunoblot Analysis. Cells were serum-starved for 6 h before drug treatments and exposed to drugs for the times and concentrations indicated. To prepare total proteins, cells were extracted in RIPA lysis buffer (50 mM Tris-HCl (pH 7.4), 150 mM NaCl, 5 mM EDTA, 5 mM EGTA, 5 mM sodium fluoride, 2 mM sodium orthovanadate, 1% NP-40, 0.1% sodium dodecyl sulfate [SDS], 1 mM phenylmethylsulfonyl fluoride [PMSF], and protein inhibitor cocktail [Roche Diagnostics, Heidelberg, Germany]). The protein concentration of the lysate was determined using the Bio-Rad dye-binding microassay. For immunoblotting, 40 μg of cell lysate was separated by SDS−polyacrylamide gel electrophoresis (PAGE). Proteins were transferred onto Hybond-ECL nitrocellulose membranes (Amersham Biosciences, Buckinghamshire, U.K.). The membranes were blocked with TBS (10 mM Tris-HCl, pH 7.4, 150 mM NaCl) containing 0.1% Tween 20 and 5% nonfat dry milk and incubated with primary antibodies diluted in blocking buffer overnight at 4 °C. The membranes were washed and incubated with the appropriate secondary antibodies for 1 h at room temperature. HRP-conjugated secondary antibodies were detected using ECL detection reagents (Amersham Biosciences, Buckinghamshire, U.K.).

AMPK Activity Assay. Total AMPK activity was measured using a synthetic SAMS peptide substrate and [γ-^{32}P]ATP, as described previously.[31] Briefly, 500 μg of protein extract was incubated with anti-AMPK-α1 and α2 antibodies for 2 h at 4 °C. Protein A/G sepharose and agarose were added, and the mixtures were incubated for 3 h at 4 °C. After the samples were washed three times with RIPA buffer, the activity was assessed in AMPK reaction buffer containing 20 mM HEPES−NaOH (pH 7.0), 0.4 mM dithiothreitol, and 0.01% Brij-35, with or without 300 μM AMP. The immune complexes were added to 23 μL of reaction buffer per assay, and then 7 μL of SAMS substrate peptide (HMRSAMSGLHLVKRR, 100 μM final concentration) and 10 μL of ATP mixture (an aliquot of 1 μCi/μL: 90 μL of 75 mM magnesium chloride, 500 μM unlabeled ATP in 20 mM MOPS, pH 7.2, 25 mM β-glycerophosphate, 5 mM EGTA, 1 mM sodium orthovanadate, and 1 mM dithiothreitol) were added, and the mixture was incubated at 30 °C for 15 min. After 35 μL was spotted onto the center of P81 paper, the paper was washed three times with 0.75% phosphoric acid and once with acetone for 5 min. The samples were read using a scintillation counter as described previously.[32]

Glucose Uptake Assay with 2-Deoxy-D-glucose-1,2-^{3}H(N). L6 myocytes were cultured in 12-well plates and incubated in low glucose medium for 16 h. The cells were washed in Kreb's Ringer phosphate (KRPH) buffer (136 mM NaCl, 20 mM HEPES, pH 7.4, 5 mM sodium phosphate, pH 7.4, 4.7 mM KCl, 1 mM $MgSO_4$, and 1 mM $CaCl_2$) and then treated with the appropriate drugs in KRPH buffer for 1 or 3 h. Next, the cells were incubated with 0.5 μCi 2-deoxy-D-glucose-1,2-^{3}H(N) for 10 min. After being washed three times with ice-cold phosphate buffered saline (PBS), the cells were lysed in 500 μL of 0.2 N NaOH and 2-deoxy-D-glucose-1,2-^{3}H(N) and counted in 5 mL of Ready Safe liquid scintillation cocktail (Beckman Coulter, USA) using a Packard 1900TR scintillation counter. When inhibitors were used, the cells were pretreated with the inhibitors for 1 h before application of the drugs.

Glucose Uptake Assay with Fluorescent Glucose Bioprobe (Cy3-Glc-α). C2C12 myocytes were cultured on a microscope cover glass in a 35 mm cell culture dish. After 2 days, the cell culture medium was removed and changed to low glucose medium (without FBS) for 4 h. The cells were incubated in glucose-depleted media (DMEM, no glucose, GIBCO) with 100 nM insulin, 10 μM AKN, and 1 mM AICAR for 1 h. Next, the medium was replaced with Cy3-Glc-α (10 μM in glucose-depleted DMEM) for 30 min. After the sample was washed three times with ice-cold phosphate buffered saline (PBS), the coverslip was loaded on the caster of a fluorescence microscope (Olympus IX71). During microscopic observation, the cells were kept in a chamber maintained at 37 °C. To monitor glucose uptake with a confocal laser scanning microscope (CLSM, Carl Zeiss-LSM510), the cover glass was loaded on the caster of the CLSM after pretreatment with the appropriate drugs for 1 h. After injection of 5 μM of Cy3-Glc-α in glucose-depleted DMEM into the chamber, a fluorescent image was taken every 7 s, digitized, and saved on the computer for analysis. The temperature of the chamber was maintained at 37 °C.

Analysis of AMP and ATP Concentration. 1×10^4 cells were seeded in 96-well plate and attached for 4 h. Cells were treated with AKN for 1 h at the indicated concentrations. ATP measurement was performed by standard protocol offered by ATPlite 1step kit (Perkin-Elmer). For the quantitative analysis of cellular AMP to ATP ratio, 1×10^6 cells were extracted in 800 μL of the extraction buffer (80% methanol) with sonication.

Then the extracts were centrifuged at 13 000 rpm for 20 min at 4 °C. The supernatants were stored at a −80 °C deep freezer until quantitative analysis was performed with HPLC−MS/MS. Electrospray ionization mass spectrometry was operated in positive ion mode using MDS Sciex API4000 triple quadrupole mass spectrometer (Applied Biosystems, Ontario, CA) followed by chromatographic separation with Agilent 1100 series HPLC system (Agilent Technologies, Palo Alto, CA) and XTerra MS C_{18} 2.1 × 150 mm, 3.5 μm column (Waters, Milford, MA, USA).

Microsomal Stability Assay. AKN was incubated with liver microsomes (human, dog, rat, and mouse) in potassium phosphate buffer. The microsomal protein concentration in the assay is 1 mg/mL, and the final percent of DMSO is 0.2%. Microsomal activity was initiated by the addition of NADPH and stopped either immediately or after 15 min for initial screening or at 15, 30, and 60 min for a more precise estimate of clearance. The corresponding loss of parent compound was determined by LC/MS. The % remaining of compound was calculated in comparison with the initial quantity at time zero. Half-life time was then calculated on the basis of first-order reaction kinetics of the % remaining of compound.

Glucose Tolerance and Insulin Stimulation Tests. After 3 weeks, glucose tolerance tests were performed in DIO mice fasted for 16 h as described previously.[33] At week 4, the mice were fasted for 4 h and ITTs were performed as described previously.[34] The animals were injected intraperitoneally with glucose (1 g/kg body weight) or human insulin (1 international unit (IU)/kg body weight), and blood glucose levels were measured.

Serum Analysis. Insulin levels in the serum of mice treated with vehicle or AKN were measured using a mouse insulin ELISA kit (ALPCO Diagnostics) according to the manufacturer's instructions. Total cholesterol, triglycerides (TG), and nonesterified free fatty acids (NEFA) in aliquoted plasma samples were determined using an automated blood chemistry analyzer (Hitachi 7150; Tokyo, Japan).

Statistical Analysis. Results were expressed as the mean ± standard deviation. Differences between groups were analyzed for statistical significance using Student's *t* test and analysis of variance (ANOVA). $P < 0.05$ was considered significant.

Acknowledgment. This study was supported by (1) the National Research Foundation of Korea (NRF); (2) the WCU program through the NRF funded by the Korean Ministry of Education, Science, and Technology (MEST); and (3) the MarineBio Technology Program funded by the Ministry of Land, Transport and Maritime Affairs (MLTM), Korea. S.O., S.J.K., H.Y.L., and J.P. are grateful for the fellowship awarded by the BK21 program, MEST, Korea. H. Y.L. and J.P. are also grateful for the predoctoral fellowship awarded of the Seoul Science Fellowship.

Supporting Information Available: Experimental procedures, spectroscopic characterization data of all new compounds, and results of biological studies. This material is available free of charge via the Internet at http://pubs.acs.org.

References

(1) Zimmet, P. Globalization, coca-colonization and the chronic disease epidemic: can the Doomsday scenario be averted? *J. Intern. Med.* **2000**, *247*, 301–310.
(2) Semenkovich, C. F. Insulin resistance and atherosclerosis. *J. Clin. Invest.* **2006**, *116*, 1813–1822.
(3) Cohen, E.; Dillin, A. The insulin paradox: aging, proteotoxicity and neurodegeneration. *Nat. Rev. Neurosci.* **2008**, *9*, 759–767.
(4) Shaw, R. J.; Lamia, K. A.; Vasquez, D.; Koo, S.-H.; Bardeesy, N.; Depinho, R. A.; Montminy, M.; Cantley, L. C. The kinase LKB1 mediates glucose homeostasis in liver and therapeutic effects of metformin. *Science* **2005**, *310*, 1642–1646.
(5) Baur, J. A.; Pearson, K. J.; Price, N. L.; Jamieson, H. A.; Lerin, C.; Kalra, A.; Prabhu, V. V.; Allard, J. S.; Lopez-Lluch, G.; Lewis, K.; Pistell, P. J.; Poosala, S.; Becker, K. G.; Boss, O.; Gwinn, D.; Wang, M.; Ramaswamy, S.; Fishbein, K. W.; Spencer, R. G.; Lakatta, E. G.; Le Couteur, D.; Shaw, R. J.; Navas, P.; Puigserver, P.; Ingram, D. K.; de Cabo, R.; Sinclair, D. A. Resveratrol improves health and survival of mice on a high-calorie diet. *Nature* **2006**, *444*, 337–342.
(6) Wing, R. R.; Goldstein, M. G.; Acton, K. J.; Birch, L. L.; Jakicic, J. M.; Sallis, J. F., Jr.; Smith-West, D.; Jeffery, R. W.; Surwit, R. S. Behavioral science research in diabetes: lifestyle changes related to obesity, eating behavior, and physical activity. *Diabetes Care* **2001**, *24*, 117–123.
(7) Hwang, J. H.; Kim, D. W.; Jo, E. J.; Kim, Y. K.; Jo, Y. S.; Park, J. H.; Yoo, S. K.; Park, M. K.; Kwak, T. H.; Kho, Y. L.; Han, J.; Choi, H.-S.; Lee, S.-H.; Kim, J. M.; Lee, I.; Kyung, T.; Jang, C.; Chung, J.; Kweon, G. R.; Shong, M. Pharmacological stimulation of NADH oxidation ameliorates obesity and related phenotypes in mice. *Diabetes* **2009**, *58*, 965–974.
(8) (a) Carling, D. The AMP-activated protein kinase cascade—a unifying system for energy control. *Trends Biochem. Sci.* **2004**, *29*, 18–24. (b) Hardie, D. G. AMP-activated protein kinase as a drug target. *Annu. Rev. Pharmacol. Toxicol.* **2007**, *47*, 185–210. (c) Hardie, D. G. Role of AMP-activated protein kinase in the metabolic syndrome and in heart disease. *FEBS Lett.* **2008**, *582*, 81–89.
(9) Shaw, R. J.; Kosmatka, M.; Bardeesy, N.; Hurley, R. L.; Witters, L. A.; DePinho, R. A.; Cantley, L. C. The tumor suppressor LKB1 kinase directly activates AMP-activated kinase and regulates apoptosis in response to energy stress. *Proc. Natl. Acad. Sci. U.S.A.* **2004**, *101*, 3329–3335.
(10) Hurley, R. L.; Anderson, K. A.; Franzone, J. M.; Kemp, B. E.; Means, A. R.; Witters, L. A. The Ca^{2+}/calmodulin-dependent protein kinase kinases are AMP-activated protein kinase kinases. *J. Biol. Chem.* **2005**, *280*, 29060–29066.
(11) Winder, W. W.; Hardie, D. G. AMP-activated protein kinase, a metabolic master switch: possible roles in type 2 diabetes. *Am. J. Physiol.* **1999**, *277*, E1–10.
(12) Treebak, J. T.; Glund, S.; Deshmukh, A.; Klein, D. K.; Long, Y. C.; Jensen, T. E.; Jørgensen, S. B.; Viollet, B.; Andersson, L.; Neumann, D.; Wallimann, T.; Richter, E. A.; Chibalin, A. V.; Zierath, J. R.; Wojtaszewski, J. F. P. AMPK-mediated AS160 phosphorylation in skeletal muscle is dependent on AMPK catalytic and regulatory subunits. *Diabetes* **2006**, *55*, 2051–2058.
(13) Hayashi, T.; Hirshman, M. F.; Kurth, E. J.; Winder, W. W.; Goodyear, L. J. Evidence for 5′ AMP-activated protein kinase mediation of the effect of muscle contraction on glucose transport. *Diabetes* **1998**, *47*, 1369–1373.
(14) Cool, B.; Zinker, B.; Chiou, W.; Kifle, L.; Cao, N.; Perham, M.; Dickinson, R.; Adler, A.; Gagne, G.; Iyengar, R.; Zhao, G.; Marsh, K.; Kym, P.; Jung, P.; Camp, H. S.; Frevert, E. Identification and characterization of a small molecule AMPK activator that treats key components of type 2 diabetes and the metabolic syndrome. *Cell Metab.* **2006**, *3*, 403–416.
(15) Stumvoll, M.; Nurjhan, N.; Perriello, G.; Dailey, G.; Gerich, J. E. Metabolic effects of metformin in non-insulin-dependent diabetes mellitus. *N. Engl. J. Med.* **1995**, *333*, 550–554.
(16) Nawrocki, A. R.; Rajala, M. W.; Tomas, E.; Pajvani, U. B.; Saha, A. K.; Trumbauer, M. E.; Pang, Z.; Chen, A. S.; Ruderman, N. B.; Chen, H.; Rossetti, L.; Scherer, P. E. Mice lacking adiponectin show decreased hepatic insulin sensitivity and reduced responsiveness to peroxisome proliferator-activated receptor γ agonists. *J. Biol. Chem.* **2006**, *281*, 2654–2660.
(17) Minokoshi, Y.; Kim, Y.-B.; Peroni, O. D.; Fryer, L. G. D.; Müller, C.; Carling, D.; Kahn, B. B. Leptin stimulates fatty-acid oxidation by activating AMP-activated protein kinase. *Nature* **2002**, *415*, 339–343.
(18) Yamauchi, T.; Kamon, J.; Minokoshi, Y.; Ito, Y.; Waki, H.; Uchida, S.; Yamashita, S.; Noda, M.; Kita, S.; Ueki, K.; Eto, K.; Akanuma, Y.; Froguel, P.; Foufelle, F.; Ferre, P.; Carling, D.; Kimura, S.; Nagai, R.; Kahn, B. B.; Kadowaki, T. Adiponectin stimulates glucose utilization and fatty-acid oxidation by activating AMP-activated protein kinase. *Nat. Med.* **2002**, *8*, 1288–1295.
(19) (a) Schreiber, S. L. Target-oriented and diversity-oriented organic synthesis in drug discovery. *Science* **2000**, *287*, 1964–1969. (b) Bruke, M. D.; Schreiber, S. L. A planning strategy for diversity-oriented synthesis. *Angew. Chem., Int. Ed.* **2004**, *43*, 46–58. (c) Tan, D. S. Diversity-oriented synthesis: exploring the intersections between chemistry and biology. *Nat. Chem. Biol.* **2005**, *1*, 74–84.
(20) (a) Ko, S. K.; Jang, H. J.; Kim, E.; Park, S. B. Concise and diversity-oriented synthesis of novel scaffolds embedded with privileged benzopyran motif. *Chem. Commun.* **2006**, 2962–2964. (b) Lee, S.-C.; Park, S. B. Novel application of Leuckart−Wallach

reaction for synthesis of tetrahydro-1,4-benzodiazepin-5-ones library. *Chem. Commun.* **2007**, 3714–3716. (c) An, H.; Eum, S. J.; Koh, M.; Lee, S. K.; Park, S. B. Diversity-oriented synthesis of privileged benzopyranyl heterocycles form s-cis-enones. *J. Org. Chem.* **2008**, *73*, 1752–1761. (d) Kim, Y.; Kim, J.; Park, S. B. Regioselective synthesis of tetrasubstituted pyrroles by 1,3-dipolar cycloaddition and spontaneous decarboxylation. *Org. Lett.* **2009**, *11*, 17–20. (e) Lee, S.; Park, S. B. An efficient one-step synthesis of heterobiaryl pyrazole[3,4-b]-pyridines via indole ring opening. *Org. Lett.* **2009**, *11*, 5214–5217.

(21) (a) Park, J.; Lee, H. Y.; Cho, M.-H.; Park, S. B. Development of a Cy3-labeled glucose bioprobe and its application in bioimaging and screening for anticancer agents. *Angew. Chem., Int. Ed.* **2007**, *46*, 2018–2022. (b) Tian, Y. S.; Lee, H. Y.; Lim, C. S.; Park, J.; Kim, H. M.; Shin, Y. N.; Kim, E. S.; Jeon, H. J.; Park, S. B.; Cho, B. R. A two-photon tracer for glucose uptake. *Angew. Chem., Int. Ed.* **2009**, *48*, 8027–8031.

(22) Cool, B.; Zinker, B.; Chiou, W.; Kifle, L.; Cao, N.; Perham, M.; Dickinson, R.; Adler, A.; Gagne, G.; Iyengar, R.; Zhao, G.; Marsh, K.; Kym, P.; Jung, P.; Camp, H. S.; Frevert, E. Identification and characterization of a small molecule AMPK activator that treats key components of type 2 diabetes and the metabolic syndrome. *Cell Metab.* **2006**, *3*, 403–416.

(23) Kim, S.-Y.; Jeoung, N. H.; Oh, C. J.; Choi, Y.-K.; Lee, H.-J.; Kim, H.-J.; Kim, J.-Y.; Hwang, J. H.; Tadi, S.; Yim, Y.-H.; Lee, K.-U.; Park, K.-G.; Huh, S.; Min, K.-N.; Jeong, K.-H.; Park, M. G.; Kwak, T. H.; Kweon, G. R.; Inukai, K.; Shong, M.; Lee, I.-K. Activation of NAD(P)H:quinone oxidoreductase 1 prevents arterial restenosis by suppressing vascular smooth muscle cell proliferation. *Circ. Res.* **2009**, *104*, 842–850.

(24) Tokumitsu, H.; Inuzuka, H.; Ishikawa, Y.; Ikeda, M.; Saji, I.; Kobayashi, R. STO-609, a specific inhibitor of the Ca^{2+}/calmodulin-dependent protein kinase kinase. *J. Biol. Chem.* **2002**, *277*, 15813–15818.

(25) Cartee, G. D.; Wojtaszewski, J. F. P. Role of Akt substrate of 160 kDa in insulin-stimulated and contraction-stimulated glucose transport. *Appl. Physiol. Nutr. Metab.* **2007**, *32*, 557–566.

(26) Kurth-Kraczek, E. J.; Hirshman, M. F.; Goodyear, L. J.; Winder, W. W. 5′ AMP-activated protein kinase activation causes GLUT4 translocation in skeletal muscle. *Diabetes* **1999**, *48*, 1667–1671.

(27) Koistinen, H. A.; Galuska, D.; Chibalin, A. V.; Yang, J.; Zierath, J. R.; Holman, G. D.; Wallberg-Henriksson, H. 5-Amino-imidazole carboxamide riboside increases glucose transport and cell-surface GLUT4 content in skeletal muscle from subjects with type 2 diabetes. *Diabetes* **2003**, *52*, 1066–1072.

(28) Hildeman, D. A.; Mitchell, T.; Kappler, J.; Marrack, P. T cell apoptosis and reactive oxygen species. *J. Clin. Invest.* **2003**, *111*, 575–581.

(29) Perriello, G.; Jorde, R.; Nurjhan, N.; Stumvoll, M.; Dailey, G.; Jenssen, T.; Bier, D. M.; Gerich, J. E. Estimation of glucose−alanine−lactate−glutamine cycles in postabsorptive humans: role of skeletal muscle. *Am. J. Physiol.* **1995**, *269*, E443–450.

(30) Goldstein, J. L.; Brown, M. S. Regulation of the mevalonate pathway. *Nature* **1990**, *343*, 425–430.

(31) Hayashi, T.; Hirshman, M. F.; Fujii, N.; Habinowski, S. A.; Witters, L. A.; Goodyear, L, J. Metabolic stress and altered glucose transport: activation of AMP-activated protein kinase as a unifying coupling mechanism. *Diabetes* **2000**, *49*, 527–531.

(32) Lee, M.; Hwang, J.-T.; Lee, H.-J.; Jung, S.-N.; Kang, I.; Chi, S.-G.; Kim, S.-S.; Ha, J. AMP-activated protein kinase activity is critical for hypoxia-inducible factor-1 transcriptional activity and its target gene expression under hypoxic conditions in DU145 cells. *J. Biol. Chem.* **2003**, *278*, 39653–39661.

(33) Abel, E. D.; Kaulbach, H. C.; Tian, R.; Hopkins, J. C. A.; Duffy, J.; Doetschman, T.; Minnemann, T.; Boers, M.-E.; Hadro, E.; Oberste-Berghaus, C.; Quist, W.; Lowell, B. B.; Ingwall, J. S.; Kahn, B. B. Cardiac hypertrophy with preserved contractile function after selective deletion of GLUT4 from the heart. *J. Clin. Invest.* **1999**, *104*, 1703–1714.

(34) Zisman, A.; Peroni, O. D.; Abel, E. D.; Michael, M. D.; Mauvais-Jarvis, F.; Lowell, B. B.; Wojtaszewski, J. F. P.; Hirshman, M. F.; Virkamaki, A.; Goodyear, L. J.; Kahn, C. R.; Kahn, B. B. Targeted disruption of the glucose transporter 4 selectively in muscle causes insulin resistance and glucose intolerance. *Nat. Med.* **2000**, *6*, 924–928.